J|A|C|S
ARTICLES
Published on Web 05/22/2004

Preparation and Characterization of Individual Peptide-Wrapped Single-Walled Carbon Nanotubes

Vasiliki Zorbas,[†] Alfonso Ortiz-Acevedo,[†] Alan B. Dalton,[‡] Mario Miki Yoshida,[§] Gregg R. Dieckmann,[†,‡] Rockford K. Draper,[†,‡,||] Ray H. Baughman,[†,‡] Miguel Jose-Yacaman,[§] and Inga H. Musselman*[,†,‡]

Contribution from the Department of Chemistry, NanoTech Institute, and Department of Molecular and Cell Biology, The University of Texas at Dallas, 2601 North Floyd Road, Richardson, Texas, 75083-0688, and Department of Chemical Engineering, The University of Texas at Austin, 1 University Station, Austin, Texas, 78712-1062

Received February 13, 2004; E-mail: imusselm@utdallas.edu

Abstract: Two challenges for effectively exploiting the remarkable properties of single-walled carbon nanotubes (SWNTs) are the isolation of intact individual nanotubes from the raw material and the assembly of these isolated SWNTs into useful structures. In this study, we present atomic force microscopy (AFM) evidence that we can isolate individual peptide-wrapped SWNTs, possibly connected end-to-end into long fibrillar structures, using an amphiphilic α-helical peptide, termed nano-1. Transmission electron microscopy (TEM) and well-resolved absorption spectral features further corroborate nano-1's ability to debundle SWNTs in aqueous solution. Peptide-assisted assembly of SWNT structures, specifically in the form of Y-, X-, and intraloop junctions, was observed in the AFM and TEM images.

Introduction

More than a decade after their discovery,[1] intense interest remains in exploiting the extraordinary electrical and mechanical properties of single-walled carbon nanotubes (SWNTs). The electrical properties of SWNTs, which range from semiconducting to metallic depending on their diameter and chirality, renders SWNTs appealing for nanowires,[2−4] rectifying heterojunctions,[5,6] field-effect transistors,[7] and nanoscale electronic devices.[8−10] Because of their high Young's modulus and aspect ratio, SWNTs can be used to make strong fibers.[11,12] The use of SWNTs in biological applications such as artificial muscles (actuators)[13,14] and biomedical sensors[15,16] are being evaluated. A major obstacle to realizing their potential is that SWNTs form parallel bundles as a result of intertube van der Waals interactions. This aggregation modifies the electronic structure of the SWNTs and complicates their dispersal, separation, and functionalization.[17]

Since most applications will require the separation and further manipulation of SWNTs, substantial effort has been placed on developing techniques to disperse and debundle SWNTs. One approach for improving SWNT dispersion is to use covalent side-wall functionalization.[18,19] Other methods include wrapping SWNTs with a wide variety of molecules, including surfactants,[20] conjugated polymers,[21,22] oligosaccharides,[23,24] and

[†] Department of Chemistry, The University of Texas at Dallas.
[‡] NanoTech Institute, The University of Texas at Dallas.
[§] Department of Chemical Engineering, The University of Texas at Austin.
[||] Department of Molecular and Cell Biology, The University of Texas at Dallas.

(1) Iijima, S. *Nature* **1991**, *354*, 56−58.
(2) Dresselhaus, M. S.; Dresselhaus, G.; Pimenta, M. *Eur. Phys. J. D* **1999**, *9*, 69−75.
(3) Cui, Y.; Wei, Q.; Park, H.; Lieber, C. M. *Science* **2001**, *293*, 1289−1292.
(4) Langer, L.; Bayot, V.; Grivei, E.; Issi, J.-P.; Heremans, J. P.; Olk, C. H.; Stockman, L.; Haesendonck, C. V.; Bruynseraede, Y. *Phys. Rev. Lett.* **1996**, *76*, 479−482.
(5) Chico, L.; Crespi, V. H.; Benedict, L. X.; Louie, S. G.; Cohen, M. L. *Phys. Rev. Lett.* **1996**, *76*, 971−974.
(6) Hu, J. T.; Min, O. Y.; Yang, P. D.; Lieber, C. M. *Nature* **1999**, *399*, 48−51.
(7) Tans, S. J.; Verschueren, A. R. M.; Dekker, C. *Nature* **1998**, *393*, 49−52.
(8) Tsukagoshi, K.; Yoneya, N.; Uryu, S.; Aoyagi, Y.; Kanda, A.; Ootuka, Y.; Alphenaar, B. W. *Physica B* **2002**, *323*, 107−114.
(9) Franklin, N. R.; Wang, Q.; Tombler, T. W.; Javey, A.; Shim, M.; Dai, H. *Appl. Phys. Lett.* **2002**, *81*, 913−915.
(10) Baughman, R. H.; Zakhidov, A. A.; de Heer, W. A. *Science* **2002**, *297*, 787−792.
(11) Vigolo, B.; Pénicaud, A.; Coulon, C.; Sauder, C.; Pailler, R.; Journet, C.; Bernier, P.; Poulin, P. *Science* **2000**, *290*, 1331−1334.
(12) Dalton, A. B.; Collins, S.; Muñoz, E.; Razal, J. M.; Ebron, V. H.; Ferraris, J. P.; Coleman, J. N.; Kim, B. G.; Baughman, R. H. *Nature* **2003**, *423*, 703.
(13) Gu, G.; Schmid, M.; Chiu, P.-W.; Minett, A.; Fraysse, J.; Kim, G.-T.; Roth, S.; Kozlov, M.; Muñoz, E.; Baughman, R. H. *Nat. Mater.* **2003**, *2*, 316−319.
(14) Baughman, R. H.; Cui, C.; Zakhidov, A. A.; Iqbal, Z.; Barisci, J. N.; Spinks, G. M.; Wallace, G. G.; Mazzoldi, A.; De Rossi, D.; Rinzler, A. G.; Jaschinski, O.; Roth, S.; Kertesz, M. *Science* **1999**, *284*, 1340−1344.
(15) Balavoine, F.; Schultz, P.; Richard, C.; Mallouh, V.; Ebbesen, T. W.; Mioskowski, C. *Angew. Chem., Int. Ed.* **1999**, *38*, 1912−1915.
(16) Chen, R. J.; Bangsaruntip, S.; Drouvalakis, K. A.; Kam, N. W. S.; Shim, M.; Li, Y.; Kim, W.; Utz, P. J.; Dai, H. *Proc. Natl. Acad. Sci. U.S.A.* **2003**, *100*, 4984−4989.
(17) Thess, A.; Lee, R.; Nikolaev, P.; Dai, H.; Petit, P.; Robert, J.; Xu, C.; Lee, Y. H.; Kim, S. G.; Rinzler, A.; Colbert, D. T.; Scuseria, G. E.; Tománek, D.; Fischer, J. E.; Smalley, R. E. *Science* **1996**, *273*, 483−487.
(18) Chattopadhyay, D.; Galeska, I.; Papadimitrakopoulos, F. *J. Am. Chem. Soc.* **2003**, *125*, 3370−3375.
(19) Boul, P. J.; Liu, J.; Mickelson, E. T.; Huffman, C. B.; Ericson, L. M.; Chiang, I. W.; Smith, K. A.; Colbert, D. T.; Hauge, R. H.; Magrave, J. L.; Smalley, R. E. *Chem. Phys. Lett.* **1999**, *310*, 367−372.
(20) Liu, J.; Rinzler, A. G.; Dai, H.; Hafner, J. H.; Bradley, R. K.; Boul, P. J.; Lu, A.; Iverson, T.; Shelimov, K.; Huffman, C. B.; Rodriguez-Macias, F.; Shon, Y.-S.; Lee, T. R.; Colbert, D. T.; Smalley, R. E. *Science* **1998**, *280*, 1253−1256.
(21) Dalton, A. B.; Stephan, C.; Coleman, J. N.; McCarthy, B.; Ajayan, P. M.; Lefrant, S.; Bernier, P.; Blau, W. J.; Byrne, H. J. *J. Phys. Chem. B* **2000**, *104*, 10012−10016.

10.1021/ja049202b CCC: $27.50 **© 2004 American Chemical Society**

biological molecules.[25,26] In previously published work, we dispersed SWNTs using a synthesized 29-residue peptide, denoted nano-1, and demonstrated that the peptide organizes SWNTs into fibrous arrays.[27] Nano-1 folds into an amphiphilic α-helix, in which apolar residues occupy one face of the helix, and more polar residues form the other face. Facilitating the dispersion of SWNTs in water using designed peptides is important for prospective biomedical and biophysical applications.

In this article, we present atomic force microscopy (AFM) evidence that we can isolate and enrich for long, individual peptide-wrapped SWNTs by using a specific sonication and centrifugation procedure. With subnanometer lateral and vertical resolution, AFM can be used to measure accurately the lengths and diameters of SWNTs. Long, individual peptide-wrapped SWNTs were observed with an average length of 1.2 ± 1.1 μm (standard deviation) and an average diameter of 2.4 ± 1.3 nm. Peptide-assisted formation of Y-, X-, and intraloop junctions was observed in AFM and transmission electron microscopy (TEM) images. Therefore, we have investigated the possibility of peptide-assisted end-to-end assembly in creating the long SWNTs. Beyond the anticipated biocompatibility benefits of peptide-wrapped SWNTs, amphiphilic peptides offer the advantage of exceptional dispersion capability, as well as the ability to form higher-ordered structures on the SWNT surface through peptide−peptide interactions.[27,28]

Experimental Section

Peptide/SWNT Sample Preparations. SWNTs produced by the method of high-pressure decomposition of carbon monoxide (HiPco process)[29] were obtained from Carbon Nanotechnologies, Inc. A 29-residue peptide, nano-1, designed to form an amphiphilic α-helix, was made using standard solid-phase peptide synthetic methods.[27] Solutions of 100 μM nano-1 were prepared using deionized water, and peptide concentrations were verified using UV−Vis absorption spectrometry (λ = 254 nm, ϵ = 788 L mol^{-1} cm^{-1}). In our previous study, we determined that 0.7 mg of SWNTs could be dispersed in 1 mL of 100 μM nano-1.[27] Therefore, to ensure a saturated dispersion, between 0.75 and 1.50 mg of HiPco SWNTs were weighed in Eppendorf tubes. To the tubes, a 1 mL volume of 100 μM nano-1 was added. The mixtures were vortexed for approximately 1 min.

Sonication was performed using a VWR Scientific Branson Sonifier 250 with the sample immersed in an ice water bath. The 2 mm diameter tip was placed into the sample approximately one-third of the distance from the surface. Samples were sonicated for either 1 or 4 min at a power level of 10 W, yielding dense black mixtures.

The sonicated samples were first centrifuged in an Eppendorf 5417C centrifuge for 10 min at 700*g*. The upper 75% of the supernatant was recovered using a small-bore pipet, avoiding sediment at the bottom, and transferred to a Beckman centrifuge tube for further centrifugation. Samples were then centrifuged for 30 min at 50000*g* in a Beckman TL-100 ultracentrifuge with the temperature controlled at 4 °C. The upper 50% of the supernatant was recovered using a small-bore pipet, avoiding sediment at the bottom, and transferred to a clean tube. High-speed centrifugation sedimented insoluble SWNTs as a pellet, yielding homogeneous gray dispersions.

This optimal centrifugation procedure was determined empirically via AFM characterization. Before selecting the 50000*g* centrifugation speed, we ultracentrifuged samples at a series of speeds. Samples were first centrifuged for 15 min at 20000*g*. The supernatant was removed and centrifuged for an additional 30 min at 50000*g*. The resulting supernatant was then removed and centrifuged for 1 h at 100000*g*. Supernatants from the 20000, 50000, and 100000*g* centrifugation steps were analyzed by AFM. The 20000*g* supernatant contained SWNTs of different sizes ranging from a few individual SWNTs to larger nanotube bundles. Very few SWNTs were present in the 100000g supernatant, indicating that they had sedimented from solution. The 50000*g* supernatant consisted primarily of long, individual SWNTs further described in this article.

The supernatants were diluted 10-fold with deionized water, and 10 μL volumes were dropped onto freshly cleaved muscovite mica (Asheville-Schoonmaker Mica Co.). Samples were placed in a desiccator to dry for 24 h prior to AFM imaging.

Peptide and SWNT Control Sample Preparations. A SWNT control sample was prepared using the same sonication and centrifugation procedure with 0.4 wt % HiPco SWNTs and 1.2 wt % sodium dodecyl sulfate (SDS) surfactant. A nano-1 control sample lacking CNTs was also prepared using an identical procedure. A lithium dodecyl sulfate (LDS)/SWNT sample was made using 0.4 wt % HiPco SWNTs and 1.2 wt % LDS using a similar procedure except for sonicating 25 min to increase SWNT concentration. Nano-1/SWNT supernatants were also diluted 10-fold with 1.2 wt % SDS and then boiled for 5 min to remove peptide from the SWNTs. Following deposition on mica, the surfactant control samples were wicked, rinsed with deionized water to remove SDS or LDS, and dried using compressed air.

Atomic Force Microscopy. AFM images were acquired in air under ambient conditions using a Digital Instruments, Inc. Nanoscope III multimode scanning probe microscope operated in the TappingMode. The AFM "J" scanner was calibrated using a NanoDevices Inc. standard consisting of lines with 2 μm pitch and 20 nm height, dimensions similar to those of SWNTs. The height calibration was verified using hydrofluoric acid-etched pits in muscovite mica, where 2 nm steps are observed along the long axis and 1 nm steps are observed along the short axis.[30] SWNT diameters were determined using AFM height measurements. Before performing a quantitative height analysis of peptide-wrapped SWNTs, silicon tip/cantilever assemblies with a range of force constants (0.9−40 N m^{-1}) (NanoDevices Inc.) were tested on a nano-1/SWNT sample to determine the effect of applied force on apparent height. A decrease in apparent height with increasing applied force was observed for the higher force constant cantilevers. Cantilevers having force constants of 0.9 and 3 N m^{-1} demonstrated minimal vertical sample compression with increasing applied force (full details available in Supporting Information). AFM images (2 × 2 μm) for height analysis of peptide-wrapped SWNTs were then acquired using a reduced Z-limit range (100 V) and cantilevers with force constants and average resonant frequencies of 0.9 N m^{-1} and 40 kHz, respectively. Larger image sizes of 10 μm were necessary for length analysis of peptide-wrapped SWNTs.

Thermogravimetric Analysis (TGA). TGA measurements of nano-1 were made to determine combustion temperature using a Perkin-Elmer Pyris 1 thermogravimetric analyzer in flowing oxygen.

(22) Dai, L.; Mau, A. W. H. *J. Phys. Chem. B* **2000**, *104*, 1891−1915.
(23) Chambers, G.; Caroll, C.; Farrell, G. F.; Dalton, A. B.; McNamara, M.; in het Panhuis, M.; Byrne, H. J. *Nano Lett.* **2003**, *3*, 843−846.
(24) Star, A.; Steuerman, D. W.; Heath, J. R.; Stoddart, J. F. *Angew. Chem., Int. Ed.* **2002**, *41*, 2508−2512.
(25) in het Panhuis, M.; Salvador, C.; Franklin, E.; Chambers, G.; Fonseca, A.; Nagy, J. B.; Blau, W. J.; Minett, A. I. *J. Nanosci. Nanotechnol.* **2003**, *3*, 210−214.
(26) Wang, S.; Humphreys, E. S.; Chung, S.-Y.; Delduco, D. F.; Lustig, S. R.; Wang, H.; Parker, K. N.; Rizzo, N. W.; Subramoney, S.; Chiang, Y.-M.; Jagota, A. *Nat. Mater.* **2003**, *2*, 196−200.
(27) Dieckmann, G. R.; Dalton, A. B.; Johnson, P. A.; Razal, J.; Chen, J.; Giordano, G. M.; Muñoz, E.; Musselman, I. H.; Baughman, R. H.; Draper, R. K. *J. Am. Chem. Soc.* **2003**, *125*, 1770−1777.
(28) Dalton, A. B.; Ortiz-Acevedo, A.; Zorbas, V.; Sampson, W.; Collins, S.; Razal, J.; Yoshida, M. M.; Baughman, R. H.; Draper, R. K.; Musselman, I. H.; Yacaman, M. J.; Dieckmann, G. R. *Adv. Funct. Mater.*, submitted for publication.
(29) Nikolaev, P.; Bronikowski, M.; Bradley, R.; Rohmund, F.; Colbert, D.; Smith, K.; Smalley, R. E. *Chem. Phys. Lett.* **1999**, *313*, 91−97.
(30) Nagahara, L. A.; Hashimoto, K.; Fujishima, A. *J. Vac. Sci. Technol., B* **1994**, *12*, 1694−1697.

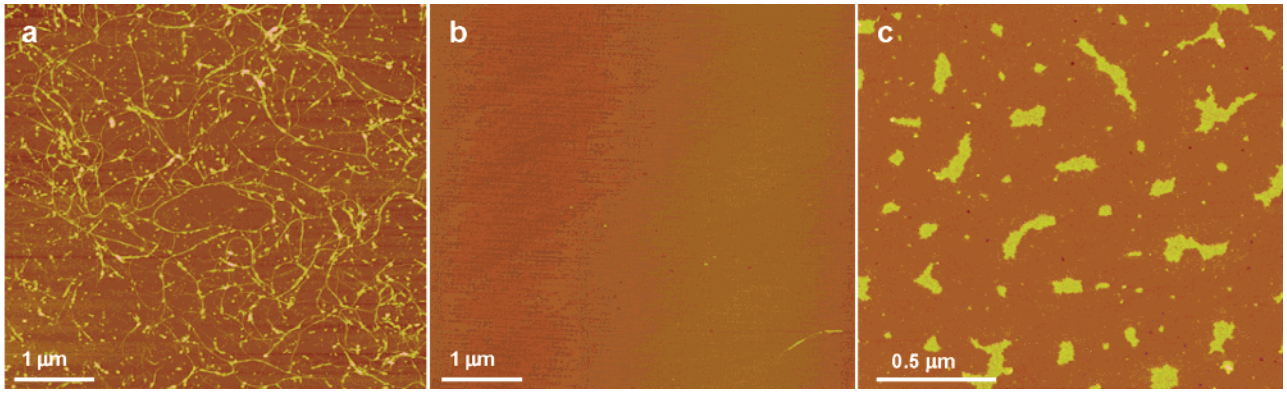

Figure 1. AFM image of nano-1/SWNT dispersion compared to SDS/SWNT and nano-1 control samples. (a) Nano-1/SWNT dispersion revealing many long SWNTs. (b) SDS/SWNT sample exhibiting minimal dispersion of SWNTs. (c) Nano-1 control sample lacking SWNTs.

Combustion Experiments. Nano-1/SWNT dispersions were prepared as previously described, and precombustion AFM images were acquired. Samples were then heated in an air atmosphere using a ThermoLyne 4800 oven at 450 °C. Samples were then placed in a desiccator for 24 h prior to acquiring postcombustion AFM images.

UV−Vis−NIR Absorption Spectrophotometry. Absorption spectra of nano-1/SWNT dispersions were obtained using a Perkin-Elmer Lamda 900 UV−Vis−NIR spectrophotometer.

Transmission Electron Microscopy. TEM images were acquired using a JEOL 2010F transmission electron microscope. High-resolution electron microscopy (HREM) and scanning transmission electron microscopy (STEM) modes were used to locate and image SWNTs. To enhance the peptide contrast, images were recorded at the optimum defocus of the objective lens at an operating voltage of 120 kV. Electron energy loss spectroscopy (EELS) was used to detect nitrogen and therefore to confirm the presence of peptide around the SWNTs. One drop of nano-1/SWNT dispersion was placed on a Cu TEM grid with holey carbon support film. The TEM grid was completely dried in air before TEM images were obtained.

Results and Discussion

AFM Length and Height Analysis. Figure 1 compares AFM images of a nano-1/SWNT sample with those of nano-1 and SWNT control samples. Unusually long SWNTs were observed in the 50000*g* nano-1/SWNT supernatant (Figure 1a). AFM images of the nano-1/SWNT dispersion, diluted 10-fold with deionized water, showed SWNTs ranging from 0.1 to 7.5 μm in length, with an average length of 1.2 ± 1.1 μm (five 10 × 10 μm images; n = 215). Although surfactant/SWNT samples sonicated for 25 min yielded black mixtures and corresponding AFM images showed several SWNTs (Figure 2b), SDS/SWNT control supernatants sonicated for 1 min yielded clear mixtures and corresponding AFM images exhibited minimal amount of SWNTs (Figure 1b). No SWNT-like features were observed in AFM images of the peptide control sample (Figure 1c).

AFM height analysis of the nano-1/SWNT dispersion revealed a diameter distribution ranging from 0.9 to 6.9 nm, with an average height of 2.4 ± 1.3 nm (four 2 × 2 μm images, n = 215) (Figure 2a). Considering that HiPco SWNTs have a diameter distribution between 0.7 and 1.4 nm, with an average diameter of approximately 1.1 nm,[29] and that the peptide coating can add an additional 1−3 nm, these height measurements suggest that the majority of the observed nanotubes are individual SWNTs wrapped with peptide. TEM images also confirm the presence of individual, peptide-wrapped SWNTs. In contrast, the height of the features in a LDS/SWNT control sample, sonicated for 25 min, ranged from 1.7 to 14.6 nm, with

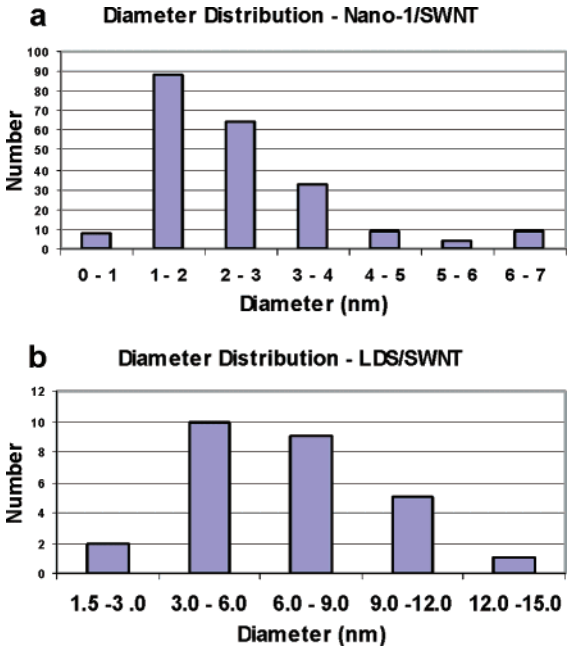

Figure 2. AFM height analysis of nano-1/SWNT dispersion compared to LDS/SWNT control. (a) Diameter distribution of nano-1/SWNT dispersion sonicated for 1 min ranged from 0.9 to 6.9 nm, average diameter = 2.4 ± 1.3 nm. (b) Diameter distribution of LDS/SWNT sample sonicated for 25 min ranged from 1.7 to 14.6 nm, average diameter = 6.6 ± 3.1 nm.

an average height of 6.6 ± 3.1 nm (three 2 × 2 μm images; n = 26) (Figure 2b). These height measurements indicate that very few, if any, of the features correspond to individual SWNTs but rather appear as nanotube bundles.

The well-resolved features in the absorption spectrum of the nano-1/SWNT dispersion (Figure 3) further demonstrate the debundling of SWNTs in aqueous solution by nano-1. The discrete peaks that extend throughout the metallic and semiconducting regions[31] indicate that under these conditions nano-1 performs well as a general dispersal agent and does not select for tubes of specific type (metallic or semiconducting).

Sonication Effects on SWNT Lengths. The dispersion of SWNTs in water using nano-1 and minimal sonication repeatedly resulted in long, individual peptide-wrapped SWNTs. Figure 4a and Table 1 illustrate nano-1's exceptional SWNT dispersion capability using a short sonication time (1 min). AFM length analysis revealed that sonicating the nano-1/SWNT

(31) Korovyanko, O. J.; Sheng, C.-X.; Vardeny, Z. V.; Dalton, A. B.; Baughman, R. H. *Phys. Rev. Lett.* **2004**, *92*, 0174031−0174034.

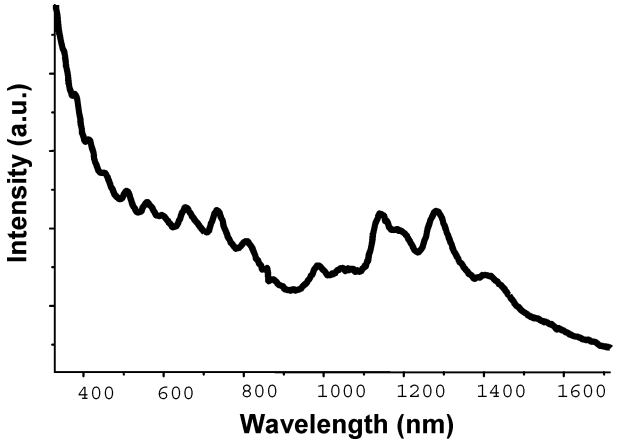

Figure 3. Absorption spectrum of a nano-1/SWNT dispersion. The well-resolved features demonstrate the ability of nano-1 to debundle SWNTs in aqueous solution. The sharp feature at ~860 nm is due to a grating and detector change associated with the spectrophotometer.

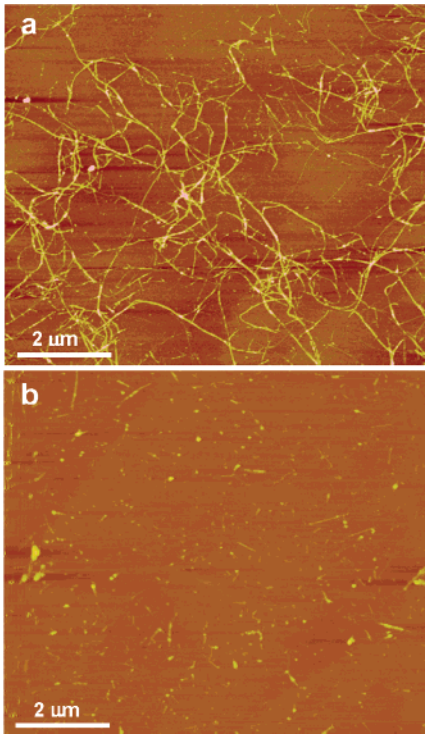

Figure 4. AFM images of a nano-1/SWNT dispersion sonicated for (a) 1 min and (b) 4 min. The longer sonication time results in shorter SWNTs.

dispersion for a longer time (4 min) severed the SWNTs. AFM images of nano-1/SWNT dispersions sonicated for 4 min showed significantly shorter SWNTs ranging from 0.1 to 1.1 μm with an average length of 0.2 $\pm$ 0.1 μm (four 10 $\times$ 10 μm images; n = 247) (Figure 4b). Standard approaches for dispersing SWNTs in common surfactants and organic solvents involve using a high-power tip sonicator for long periods of time (~15 min to 1 h).[32,33] The longer sonication times required for adequate dispersion inevitably result in tube breakage. Sonication in a low-power bath sonicator for ~16−24 h has been reported to reduce tube breakage but still yields approximate average lengths of 500 nm.[34] The short sonication time and superior dispersing capability of nano-1 compared to other surfactants such as SDS (≤0.1 mg/mL) and Triton-X 100 (≤0.5 mg/mL) are the result of designing amphiphilic peptides to interact with SWNTs. While there are few reports of the noncovalent immobilization of water-soluble proteins on SWNT surfaces,[35] previous studies involving the development of fullerene-specific antibodies suggest that proteins utilize π-stacking interactions between the fullerene and the aromatic side chains of the amino acids Tyr, Trp, and Phe.[36,37] We therefore suspect that the π-stacking ability of the aromatic amino acids in nano-1 with the graphite surface of the SWNT enhances the dispersing capability of nano-1 over surfactants that have weaker interactions with the SWNT surface. Nano-1's ability to disperse SWNTs with minimal sonication time avoids substantial breakage of these long SWNTs.

Table 1. Comparison of SWNT Density in 1-min Sonicated Nano-1/SWNT and SDS/SWNT Samples

nano-1/SWNT		SDS/SWNT	
image area	No. of CNTs	image area	No. of CNTs
10 × 10 μm	74	10 × 10 μm	0
10 × 10 μm	51	20 × 20 μm	1
10 × 10 μm	64	20 × 20 μm	1
5 × 5 μm	28	15 × 15 μm	1
325 μm^2 total area	217	1125 μm^2 total area	3

Peptide−Peptide Interactions. Besides the sonication and centrifugation factors for enriching the yield of long, individual SWNTs, peptide−peptide interactions may also assist in the assembly of SWNT structures. Various junctions and "beads" of peptide are evident in the AFM images of nano-1/SWNT dispersions. It has been reported that less than 2% of pristine SWNTs exhibit junctions, while 30% of functionalized SWNTs form junctions by molecular linkers.[38] Statistical analysis of nanotube features in AFM images of nano-1/SWNT dispersions (identified in Table 1) shows that 25% of the SWNTs participate in junctions: 14% are Y, 8% are X, and 3% are intraloop conformations (AFM images in Supporting Information). The arrow in Figure 5a provides an example of a peptide-assisted X-junction where one SWNT has an approximate diameter of 1.8 nm and a second SWNT has an approximate diameter of 2.6 nm before and after the junction. An elevated height of 6.4 nm at the junction demonstrates that the SWNTs are not just overlapping but that the peptide interconnects the two SWNTs. The HREM structural image in Figure 5b provides a detailed view of the peptide-assisted formation of a Y-junction in a nano-1/SWNT dispersion. The junctions observed in nano-1/SWNT dispersions are consistent with the structure of folded nano-1, which was designed to promote self-assembly through peptide−peptide interactions.[27] The junctions could easily be formed by helical peptides that bridge adjacent SWNTs.

(32) O'Connell, M. J.; Bachilo, S. M.; Huffman, C. B.; Moore, V. C.; Strano, M. S.; Haroz, E. H.; Rialon, K. L.; Boul, P. J.; Noon, W. H.; Kittrell, C.; Ma, J.; Hauge, R. H.; Weisman, R. B.; Smalley, R. E. *Science* **2002**, *297*, 593−596.
(33) Bahr, J. L.; Mickelson, E. T.; Bronikowski, M. J.; Smalley, R. E.; Tour, J. M. *Chem. Commun.* **2001**, *2*, 193−194.
(34) Islam, M. F.; Rojas, E.; Bergey, D. M.; Johnson, A. T.; Yodh, A. G. *Nano Lett.* **2003**, *3*, 269−273.
(35) Chen, R. J.; Zhang, Y.; Wang, D.; Dai, H. *J. Am. Chem. Soc.* **2001**, *123*, 3838−3839.
(36) Braden, B. C.; Goldbaum, F. A.; Chen, B.-X.; Kirschner, A. N.; Wilson, S. R.; Erlanger, B. F. *Proc. Natl. Acad. Sci. U.S.A.* **2000**, *97*, 12193−12197.
(37) Erlanger, B. F.; Chen, B.-X.; Zhu, M.; Brus, L. *Nano Lett.* **2003**, *1*, 465−467.
(38) Chiu, P. W.; Duesberg, G. S.; Dettlaff-Weglikowska, U.; Roth, S. *Appl. Phys. Lett.* **2002**, *80*, 3811−3813.

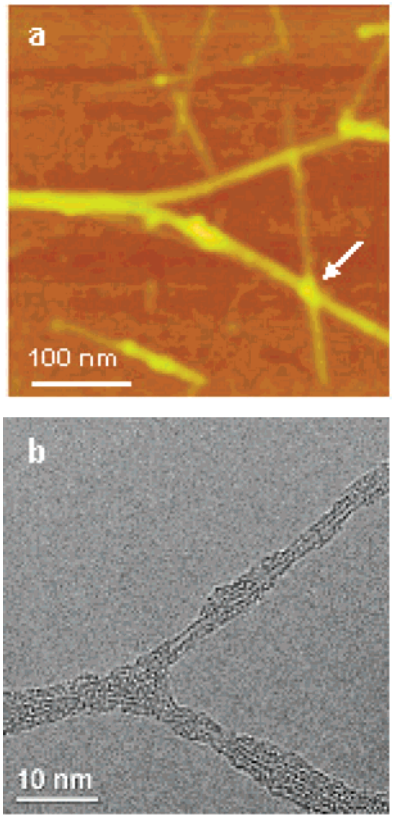

Figure 5. (a) AFM image of nano-1/SWNT sample exhibiting a Y-junction and an X-junction (arrow). (b) TEM image of peptide-coated SWNTs exhibiting Y-junction apparently created through peptide−peptide interactions.

AFM images of the peptide control samples (Figure 1c) demonstrate that the nano-1 does not form fibrillar structures with itself. Yet, if the peptide can assist in the assembly of SWNT structures, such as X- and Y-junctions, it may also facilitate end-to-end polymerization of short SWNTs to create the unusually long SWNTs we observe. To decipher if peptide "beads", observed along the length of a nanotube, are connecting individual SWNTs into longer fibrillar structures, nano-1/SWNT samples were heated in air with the intention of removing peptide. TGA results indicate that the combusting temperature of nano-1 is 450 °C. After the SWNTs were heated in air at 450 °C for 2 h, AFM postcombustion images reveal a network of long SWNTs that clearly demonstrate diminished peptide "beading" compared to precombustion images of the same sample (Figure 6). AFM height analysis revealed that most of the peptide was removed as a result of heating. AFM height measurements (diameter) of SWNTs in precombustion images ranged from 0.8 to 10.0 nm with an average diameter of 2.1 ± 1.7 nm, and SWNT diameters in postcombustion images ranged from 0.7 to 3.3 nm with an average diameter of 1.0 ± 0.4 nm (details in Supporting Information). The presence of these long fibrillar structures, exhibiting diameters consistent with those of individual SWNTs upon the removal of peptide, suggests that extraordinarily long SWNTs are indeed being isolated with our procedure.

To further investigate the possibility that peptide connects SWNTs end-to-end, the nano-1/SWNT dispersions were diluted 10-fold with 1.2 wt % SDS and then boiled for 5 min to remove the peptide from the SWNTs. Figure 7 shows the presence of long SWNTs and an absence of tube junctions upon the removal of peptide (large white spots are likely removed peptide). However, a nonuniform thickness along the length of the SWNTs suggests that peptide may still be present. Diameters ranged from 0.8 to 2.8 nm with an average diameter of 1.3 ± 0.6 nm ($n = 60$, measurements taken at ∼300 nm intervals along nine SWNTs). The irregularity of SWNT diameters, however, could also be due to the presence of SDS.

While it is possible that peptide connects SWNTs into long fibrillar structures, these data overall point toward our ability to isolate long, individual SWNTs using designed, amphiphilic peptides and a specific sonication and centrifugation procedure.

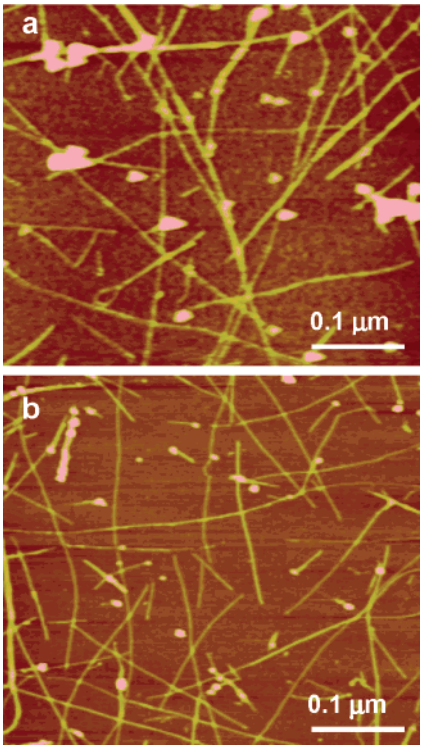

Figure 6. A nano-1/SWNT sample was heated in air to remove peptide. AFM images of a nano-1/SWNT dispersion (a) precombustion and (b) postcombustion at 450 °C for 2 h. Long SWNTs remain while peptide significantly diminishes.

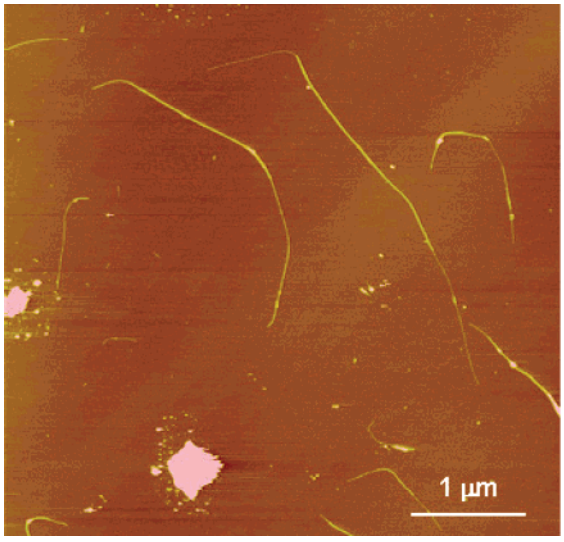

Figure 7. AFM image of nano-1/SWNT sample diluted 10-fold with 1.2 wt % SDS and then boiled to remove peptide from SWNTs. Long SWNTs are present, and tube junctions are absent upon peptide removal.

We hypothesize that by altering the properties of the solubilizing peptide, the properties of the peptide/SWNT composites can be manipulated.

Conclusions

We have demonstrated the ability to isolate individual peptide-wrapped SWNTs, possibly assembled into longer structures through peptide−peptide interactions, using a specific sonication and centrifugation procedure. Peptide−peptide interactions apparently assist in the assembly of SWNT structures, specifically in the formation of Y-, X-, and intraloop junctions. Although the possibility of peptide-assisted end-to-end SWNT assembly cannot be ruled out, combustion and SDS experiments conducted to remove the peptide from the SWNTs suggest that truly long SWNTs are isolated using the designed amphiphilic peptide.

Peptide/SWNT dispersions extend the already vast list of prospective applications of SWNTs to comprise disease diagnostics and nanobiotechnologies. The use of these peptide-coated SWNTs is by no means limited solely to biophysical or biomedical applications. Bridging SWNTs with peptides spawns new ways for the dispersion and manipulation of SWNTs. Research is currently underway to extend the design of peptides with enhanced nanotube affinities and self-assembly properties for the generation of useful architectures.

Acknowledgment. The support of this research by the Robert A. Welch Foundation [AT-1326 (I.H.M.), AT-1448 (G.R.D.)] and the Department of Homeland Security (V.Z.) are gratefully acknowledged. We would like to thank Chong-Min Fu and Amy Smith for general assistance.

Supporting Information Available: Experimental details and results of a study of AFM height measurements on a nano-1/SWNT sample as a function of applied force, pre- and postcombustion AFM height (SWNT diameter) measurements, and AFM images of intraloop junctions (PDF). This material is available free of charge via the Internet at http://pubs.acs.org.

JA049202B